Assessment of Uncertainties in Eddy Covariance Flux Measurement Based on Intensive Flux Matrix of HiWATER-MUSOEXE

Jiemin Wang, Jinxin Zhuang, Weizhen Wang, Shaomin Liu, and Ziwei Xu

Abstract—To study the multiscale characteristics of ecohydrological processes in the Heihe River Basin, an intensive flux observation matrix was established, which consisted of mainly 17 eddy covariance (EC) flux stations in a 5.5 km $\times$ 5.5 km area of the Zhangye oasis. Formal observations began in June and continued through September 2012. Before the main campaign, an intercomparison for all instruments (including 20 EC sets) was conducted in the Gobi desert. All the data provided a rare opportunity to assess the flux uncertainties of EC measurements. Three methods were chosen in this assessment. For the Gobi intercomparison, a simple method based on elementary error analysis could provide the systematic errors and random uncertainties for each EC; uncertainties for sensible heat flux were generally less than 10% in this area. For flux matrix observations, by using mainly the method of Mann and Lenschow (1994), the uncertainties estimated for sensible heat, latent heat, and CO_2 fluxes were approximately 18%, 16%, and 21%, respectively, for the selected period. These were comparatively high because of the inherent heterogeneities of the oasis. The flux uncertainty quantification, including its probability distribution and the nonconstant variance characteristics shown for these data sets, is essential for flux data interpretation and applications, particularly the validation of relevant remote sensing models.

Index Terms—Eddy covariance (EC), land surface, measurement uncertainty, turbulent fluxes.

I. INTRODUCTION

EDDY covariance (EC) is generally the most accurate and reliable method to measure heat, water vapor, and CO_2 fluxes between land surfaces and atmosphere at the ecosystem scale. It is now the basis of global micrometeorological measurement networks [1], as well as fundamental in numerous land surface process experiments, such as the recent project Heihe Watershed Allied Telemetry Experimental Research (HiWATER) and its subproject Multiscale Observation Exper-

iment on Evapotranspiration (MUSOEXE) conducted in the Heihe River Basin, northwest China [2], [3].

Flux measurements by the eddy covariance (EC) method are also subject to errors. A landmark paper by Lenschow *et al.* [4] has defined systematic and random errors associated with limited samplings of the EC measurements. Subsequently, as the extensive use of EC systems, a number of papers have been published on this aspect [5]–[7]; several methods have emerged for flux uncertainty estimation accordingly [8]–[11]. However, various problems are still under discussion. Contrary to traditional error analysis, which has a long history in physics and engineering, the assessment of EC flux errors is more difficult. The systematic errors are not only instrument-related but also affected by the unmet environmental conditions of the EC theory, and its data processing scheme that is actually a complex, long sequence of operation. Moreover, flux exchange is controlled by atmospheric turbulence, which is an inherently random process. Flux data often show "wiggly" variations in consecutive half-hour sequences, even in a clear stationary day when the net radiation shows a typical smooth diurnal cycle. These random uncertainties primarily arise due to a limited number of independent samples of the turbulent eddies responsible for flux transport during a fixed sampling period [4]. Other errors can be greatly reduced in a carefully designed field program; however, these "sampling error" will remain as one of the largest sources of uncertainty.

The normalized sampling error may range from 10% for sensible heat to 25%–30% for trace gases [9]. These rather large errors should be kept in mind in the flux data interpretation and analysis. When scaling up fluxes spatially or temporally to obtain, for example, the total evapotranspiration (ET) or annual CO_2 sequestration of a specific area, knowing the uncertainty of the relevant flux is critical. More importantly, this information is fundamental for the validation and optimization of relevant hydrological, ecological, and/or remote sensing models. Data uncertainties are entered directly into the "model–data fusion" (MDF); thus, incorrect data uncertainties affect the parameter estimates and propagate into the model predictions [12].

A comprehensive review or deep theoretical analysis of the methods used to quantify EC flux uncertainties is beyond the scope of this letter. Rather, we intend to make a critical examination of the flux uncertainties (mainly the sampling errors), based on our unique and intensive flux observation matrix in the MUSOEXE. Equally important is the pre-main-campaign intercomparison for all the EC systems in the Gobi desert. Since there is no absolute standard or more precise method for measuring fluxes, this multiple independent EC observations in one

J. Wang, J. Zhuang, and W. Wang are with the Cold and Arid Regions Environmental and Engineering Research Institute, Chinese Academy of Sciences, Lanzhou 730000, China (e-mail: jmwang@lzb.ac.cn; zhgis@163.com; weizhen@lzb.ac.cn).

S. Liu and Z. Xu are with the State Key Laboratory of Remote Sensing Science, School of Geography, Beijing Normal University, Beijing 100875, China (e-mail: smliu@bnu.edu.cn; xuzw@bnu.edu.cn).

simpler surface could evaluate the systematic and random errors for each EC, as well as the methods used for random uncertainty assessment. It is expected to provide these results for a better utilization of the flux data and, finally, a better understanding of multiscale processes in this heterogeneous watershed.

II. EXPERIMENTS AND DATA PROCESSING

A. Intercomparison of Flux Measurement Systems

An intercomparison campaign for all of the flux systems was conducted in the Gobi desert ($100°18'15.17''$E; $38°54'53.87''$N) from May 14 to 24, 2012, immediately prior to the start of the formal observations. The area is open and comparatively flat and homogeneous.

Twenty sets of EC systems, including 1 set of CSAT3 + EC150 (by Campbell Sci. Inc., USA), 16 sets of CSAT3 + LI-7500/7500A (by LI-COR, USA), and 3 sets of Gill-WM (by Gill Inst. Ltd., U.K.) + LI-7500/7500A, were installed 1.7 m high, facing north (the prevailing wind direction), and separated by approximately 0.7 m.

Moreover, seven sets of large aperture scintillometers (LASs) and 18 sets of radiometers were installed in proximity.

All of the instruments were maintained and calibrated before the installation. Detailed information of the layout of the Gobi intercomparison can be found in Xu *et al.* [3].

B. HiWATER-MUSOEXE Flux Matrix

The formal observation of HiWATER-MUSOEXE was primarily performed by a flux matrix in the middle reach of the Heihe River Basin. The flux matrix was specifically designed to obtain high-accuracy ET data and be used in combination with remote sensing and other model products to capture the multiscale characteristics of a heterogeneous landscape. The kernel experimental area was approximately 5.5 km × 5.5 km (centered at approximately $100°22'$E, $38°52'$N) in the Zhangye oasis. As shown by the numbers 1–17 in Fig. 1, 17 elementary sampling plots were selected according to their crop structures and landscape status. Each site had an observation tower with an EC system (placed at a height of approximately 3–7 m), and the necessary micrometeorological observations (four-component radiation, one to two levels wind/temperature/humidity profile, soil temperature/moisture profile and heat flux, etc.). Among the sites, site 15 was a superstation equipped with a 40-m tower, two-level EC system (4.5 and 30 m), and seven-level profiles. In the middle of the kernel observation area, a 3 km × 3 km grid coincided with MODIS pixels for the intercomparison with relevant remote sensing products. Four paths of LAS observations crossed over the district are also shown in Fig. 1. The observational experiments were conducted from June to September 2012.

Except for sites 1 (vegetable field), 4 (residential area), and 17 (orchard), all other sites were in the corn field (corn for seed). The crops were seeded in early May and synchronously grew in these sites until mid-September.

C. Data Processing and Quality Control

All of the flux data were processed on the basis of a 30-min time step. Proper data processing and quality control pro-
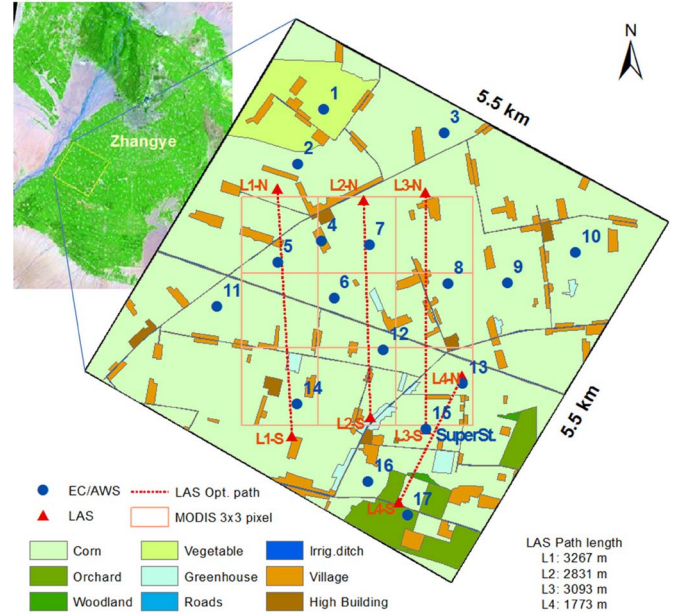

Fig. 1. Flux matrix in the Zhangye oasis, which included 17 EC sites and four LAS lines in a 5.5 km × 5.5 km area.

cedures are essential to reduce the systematic and random errors of the EC fluxes. The software package EddyPro ver. 4.2.1 (www.licor.com/eddypro) was applied, and the following workflow was adopted.

1) The raw turbulence data were screened, including spike removal, angle of attack correction (for Gill), checking for absolute limits, skewness and kurtosis, discontinuities, etc.
2) The ECs were then calculated, which included the necessary corrections for sonic head tilt, sonic virtual temperature, Webb-Pearman-Leuning (WPL), and spectral losses.
3) A quality assessment was performed using the flag system (0, 1, and 2). The data of flag 2 were discarded, and mostly, the data of highest quality with flag 0 were used in this study.

III. METHODS OF UNCERTAINTY ASSESSMENT

For the Gobi intercomparison, a simple method based on elementary error analysis could be used. In addition, other two widely used methods were adopted.

1) Method Based on Elementary Error Analysis: During a measurement, if the actual ("*true*") value $\dot{F}$ was obtained, such as by calibration with a "standard" instrument, and the observed value in the experiment was F, then the total observation error was $\Delta F \stackrel{\text{def}}{=} F - \dot{F}$. The system error (bias) can be estimated as

$$\Delta F_s = E[\Delta F] \approx \overline{\Delta F} = \frac{1}{N}\Sigma_{i=1}^{N}\Delta F_i. \qquad (1)$$

The random error $\Delta F_r \stackrel{\text{def}}{=} \Delta F - \Delta F_s$ was normally characterized by the variance σ^2 (σ =standard deviation), i.e.,

$$\sigma^2 = E\left[(\Delta F_r)^2\right] \approx \frac{1}{N-1}\Sigma_{i=1}^{N}(\Delta F_i - \overline{\Delta F})^2. \qquad (2)$$

On the other hand, if the predicted value determined by linear regression was $\hat{F}$, then according to Willmott [13], the total error σ_T^2 can be partitioned between its systematic σ_s^2 and random σ_r^2 components, i.e.,

$$\sigma_T^2 = \sigma_s^2 + \sigma_r^2. \tag{3}$$

The components were defined by

$$\begin{cases} \sigma_T^2 = \sigma^2(F - \dot{F}) \\ \sigma_s^2 = \sigma^2(\hat{F} - \dot{F}) \\ \sigma_r^2 = \sigma^2(F - \hat{F}). \end{cases} \tag{4}$$

2) Method of Mann and Lenschow [8] (hereafter, ML94): This method was developed based on a statistical analysis of the turbulent transport process. Mann and Lenschow showed that the relative flux uncertainty from pure random sampling error is

$$\frac{\sigma_r(\tau)}{|F|} = \left(\frac{2\tau_f}{\tau}\right)^{0.5} \left(\frac{1 + r_{wx}^2}{r_{wx}^2}\right)^{0.5} \tag{5}$$

where τ_f is the integral time scale of the measurement; T is the averaging period; and r_{wx} is the correlation coefficient between vertical velocity w and scalar x.

3) Paired Tower Method of Hollinger and Richardson [10] (hereafter, HR05): For two collocated but independent measurements of flux F, the uncertainty can be calculated as

$$\sigma_r = \frac{1}{\sqrt{2}} \left[\sigma^2(F_2 - F_1)\right]^{\frac{1}{2}}. \tag{6}$$

This approach requires that the observations of the two towers be "similar" (for both instruments and environmental conditions) and "independent" (with nonoverlapping footprints). The "similar" condition here implies that the "systematic errors" are almost ignorable, and the results evaluated by (6) are primarily "random errors" controlled by atmospheric turbulence. Some authors have used equations similar to (6) for two nearly separated (e.g., by approximately 1 m as in Dragoni *et al.* [14]) EC systems. Thus, the two ECs are exposed to essentially the same eddies that contribute to the flux, and only the "random instrument errors" are quantified.

IV. RESULTS

A. Errors and Uncertainties for the Gobi Intercomparison

As aforementioned, the intercomparison campaign was conducted in an open, flat, and homogeneous region of the Gobi desert that had a dry surface and sparse vegetation (Alhagi gagnebin, which was also dry in May). ET and CO_2 flux were comparatively very small [3]. Thus, we only focus here on the error and uncertainty analysis of sensible heat flux. Due to the close positioning of the EC sensors, method HR05 was not used.

In order to reduce the flow distortion induced by neighboring sensors, only the 30-min data with a wind direction in the northern sector ($280°-0°-80°$) were selected. Combined with the selections from the quality control (QC) flags, acceptable flux data obtained were a total of 166 30-min runs.

TABLE I
SYSTEMATIC AND RANDOM ERRORS ESTIMATED BY ELEMENTARY ERROR ANALYSIS FOR SENSIBLE HEAT FLUXES H (W/m^2) DURING THE GOBI INTERCOMPARISON. THE RESULTS FROM (1) AND (2) AND FROM (3) AND (4) ARE BOTH SHOWN (RELATIVE ERRORS SHOWN IN PARENTHESES). THE LAST COLUMN SHOWS THE RESULTS FROM METHOD ML94

EC No.	$\bar{H}$	Eq. (1) & (2)		Eq. (3) & (4)		ML94
		$\overline{\Delta H}$	σ_r	σ_s	σ_r	σ_r
1	97.07	3.38	9.72	4.37 (5%)	8.68 (9%)	9.48 (10%)
2	96.60	3.33	9.67	3.21 (3%)	9.12 (9%)	9.26 (10%)
3	96.53	1.56	7.97	0.75 (1%)	7.94 (8%)	8.81 (9%)
4	96.22	1.32	11.11	1.45 (2%)	11.01 (11%)	8.99 (9%)
5	67.70	-0.91	7.20	0.12 (0%)	7.20 (11%)	7.07 (10%)
6	79.51	-0.81	7.14	1.09 (1%)	7.06 (9%)	7.72 (10%)
7	93.82	-1.89	8.62	1.57 (2%)	8.47 (9%)	8.94 (10%)
8	82.16	-3.77	7.97	3.74 (5%)	7.04 (9%)	7.96 (10%)
9	87.47	1.32	7.25	0.59 (1%)	7.23 (8%)	8.53 (10%)
10	87.44	2.12	13.05	0.15 (0%)	13.05 (15%)	8.49 (10%)
11	78.10	0.09	8.16	0.43 (1%)	8.15 (10%)	7.95 (10%)
12	95.53	-1.12	8.04	0.72 (1%)	8.01 (8%)	9.03 (9%)
13	93.60	-0.92	7.49	2.50 (3%)	6.91 (7%)	8.82 (9%)
14	94.94	-0.76	8.93	0.84 (1%)	8.89 (9%)	9.11 (10%)
15	97.76	0.41	10.61	0.97 (1%)	10.56 (11%)	9.36 (10%)
16	67.60	-3.25	8.38	1.08 (2%)	8.31 (12%)	7.26 (11%)
17	93.27	-1.41	7.89	1.81 (2%)	7.68 (8%)	5.86 (6%)
18	89.30	-2.27	8.10	2.57 (3%)	7.69 (9%)	8.47 (9%)
19	71.05	-6.41	10.81	5.47 (8%)	9.32 (13%)	7.11 (10%)
20	92.01	8.68	12.14	7.45 (8%)	9.58 (10%)	9.80 (11%)

1) "True" Fluxes: Among the 20 EC sets for intercomparison, six CSAT3's and two Gill-WM's were brand new (calibrated by the manufactures). The comparison by linear regressions of the mean sensible heat flux H from the six new CSAT3's, all the eight new sonic's, and all the 20 EC sets showed that they were all consistent (slope $\approx 0.99-1.01$ and $R^2 = 1.00$). The "energy balance closure" over the desert surface is normally good; thus, fluxes measured by the EC method over this rather simple surface should be highly accurate. It is reasonable to assume that the mean H of the 20 EC sets, which were working simultaneously, can be regarded as the "*true*" flux.

This assumption was proven by the simultaneous and independent measurements of the scintillometers. A linear regression between the mean heat flux from the ECs and that from LASs showed a slope of 1.01 and $R^2 = 0.96$. The agreement was as good as expected.

2) Results by Elementary Error Analysis: If the "*true*" flux is known, then based on flux data samples and the methods mentioned in Section III-A1, we can calculate the systematic and random errors for each EC and the random errors for each time step. As shown in Table I and Fig. 2, except for a few sets, the systematic errors $\overline{\Delta H}$ and σ_s diverged from the mean heat flux $\bar{H}$ by only several watts per square meter or percent points. Random errors σ_r are obviously larger than systematic errors as expected; however, they were still mostly within 10%. Table I and Fig. 2 also showed that the systematic and random errors from simple error estimation [see (1) and
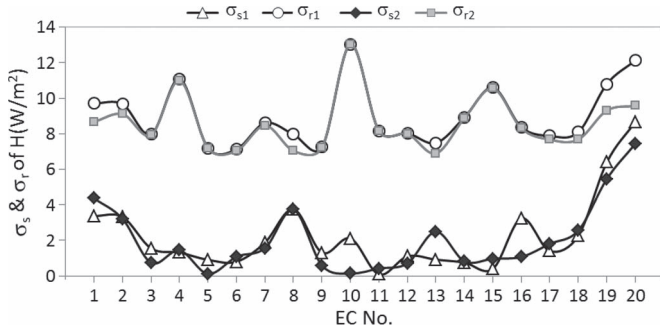
Fig. 2. Error partitioning by simple calculation from (1) and (2) (subscript 1, $\sigma_{s1} = |\overline{\Delta H}|$) and Willmott's method from (3) and (4), (subscript 2).
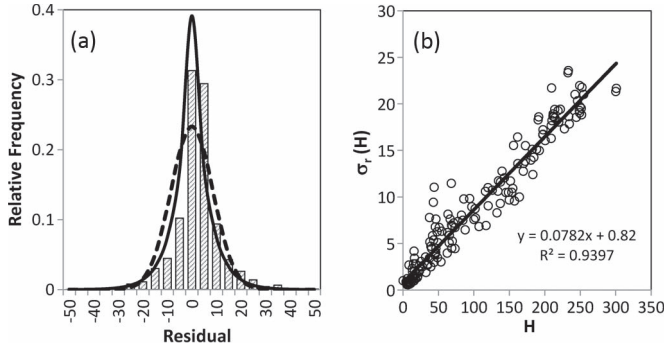

Fig. 3. Uncertainties of the sensible heat flux in the Gobi intercomparison. (a) Distribution of the residuals from the mean (skewness = 0.72). A Laplace distribution (full line, $\beta = 6.05$) and a Gaussian distribution (dash line, $\mu = 0$, $\sigma = 8.56$) are added for comparison. (b) Linear regression of the random uncertainties by method ML94 with the mean values of sensible heat (H, W/m^2).

(2)] and from Willmott's separation [see (3) and (4)] agreed well, respectively.

This analysis was helpful for the flux matrix configuration and data quality control. For instance, EC sets with larger systematic error (e.g., numbers 19 and 20) were not installed in the middle parts of the kernel observation area.

3) In the assessment of model validity and study of the propagation of observation errors into model outputs, a probability model (such as Bayes' theorem) is usually used to quantify the model uncertainties. Thus, a probability density function (pdf) of the random errors of the surface measurement would be required. Generally, a non-Gaussian but double exponential pdf (Laplace distribution) better characterizes the uncertainty of EC fluxes [5]. Fig. 3(a) shows the frequency distribution of random errors in the Gobi intercomparison. A Laplace distribution $f(x) = \exp(-|x/\beta|)/2\beta$ (where $\beta = \overline{|\Delta H|}$) and a Gaussian distribution were added for comparison. The data better fit the double exponential distribution than the Gaussian. However, skewness was also apparent, which was found in other sites as well [5], [10].

4) Results by method ML94: Based on the raw turbulence records of each 30-min step, (5) was used to calculate the (random) uncertainty of the sensible heat flux. The results for each EC set are shown in the last column of Table I. This method was clearly consistent with the elementary error analysis.

5) Many studies have demonstrated that uncertainty increases with the magnitude of the flux (nonconstant variance) [5],

TABLE II
UNCERTAINTY ESTIMATES FROM ML94 FOR THE FLUXES OF SENSIBLE HEAT $\sigma_r(H)$ (W/m^2), LATENT HEAT $\sigma_r(LE)$ (W/m^2), AND CARBON DIOXIDE $\sigma_r(Fc)$ (μmol/m$^2 \cdot$ s) FOR EACH OF THE 14 CORN FIELD SITES DURING JUNE 7–16, 2012

Site No.	$\sigma_r(H)$	$\sigma_r(LE)$	$\sigma_r(Fc)$
2	10.56 (17.6%)	31.85 (13.7%)	2.59 (18.1%)
3	14.37 (18.9%)	33.86 (15.4%)	2.40 (21.7%)
5	9.98 (16.0%)	26.45 (14.3%)	2.00 (20.4%)
6	13.66 (16.1%)	30.53 (15.9%)	2.13 (27.7%)
7	9.26 (21.2%)	33.57 (14.3%)	2.59 (18.7%)
8	10.31 (17.6%)	29.48 (14.9%)	2.10 (21.3%)
9	13.47 (16.6%)	28.82 (15.4%)	3.03 (20.7%)
10	12.62 (17.7%)	30.9 (15.2%)	3.12 (19.3%)
11	12.21 (15.2%)	26.94 (14.8%)	2.48 (20.0%)
12	10.34 (20.3%)	32.62 (16.1%)	2.40 (22.2%)
13	10.33 (25.0%)	43.13 (17.8%)	3.11 (29.9%)
14	14.62 (17.8%)	35.96 (16.6%)	2.58 (25.8%)
15	10.60 (21.1%)	33.78 (16.2%)	2.49 (21.8%)
16	11.43 (16.3%)	22.17 (16.7%)	2.18 (22.8%)

which also occurred in our observations. A linear regression test for the Gobi heat fluxes is shown in Fig. 3(b).

B. Errors and Uncertainties for Flux Matrix on Oasis

As mentioned in Section II-B (see Fig. 1), 14 sites (2, 3, 5, 6, 7, 8, 9, 10, 11, 12, 13, 14, 15, and 16) were in the corn fields. Their landscapes were very similar. However, occasional rains and irregular irrigations would cause soil moisture inhomogeneity in this oasis area. In order to focus on the impacts of the atmospheric turbulence on the flux uncertainties, ten continuous days (June 7–16, with a crop height of approximately 0.5 m) in which there were no rain or irrigation in the plots were selected for this analysis. The quality controls mentioned in Section II-C were also adopted.

1) Uncertainty Assessed by Method ML94: For the selected days, the uncertainty estimates for the fluxes of sensible heat $\sigma_r(H)$ (W/m^2), latent heat $\sigma_r(LE)$ (W/m^2), and carbon dioxide $\sigma_r(Fc)$ (μmol/m$^2 \cdot$ s) for each of the 14 corn field sites are depicted in Table II. Compared with the Gobi intercomparison, the uncertainties in the oasis were obviously larger, particularly for the sensible heat flux. The uncertainties of latent heat flux for the 14 sites were comparatively uniform, whereas the uncertainties of sensible heat and CO_2 fluxes were rather scattered among the different sites. On average, the uncertainties for H, LE, and Fc were approximately 18%, 16%, and 21%, respectively.

As aforementioned [see Fig. 3(b)], the uncertainty increases with the flux magnitude. Fig. 4 illustrates the scatter graphs for H, LE, and Fc, as well as the linear regression parameters. The intercept indicates a baseline uncertainty when the relevant flux tends to be zero. Obviously, the relative uncertainties are comparatively much larger when the mean fluxes are small or close to zero. This would explain the comparatively larger uncertainties for sensible heat and CO_2 fluxes on these oasis sites. As the fluxes become larger, the uncertainties for H, LE, and Fc would tend to be approximately 14%, 13%, and 16%, respectively.
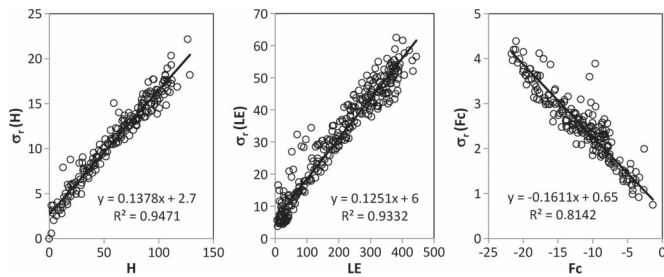
Fig. 4. Linear regressions of the random uncertainties by the ML94 method with the mean values of sensible heat (H, W/m^2), latent heat (LE, W/m^2), and carbon dioxide (Fc, μmol/m$^2 \cdot$ s).

TABLE III
UNCERTAINTIES FOR SENSIBLE HEAT, LATENT HEAT, AND CO$_2$ FLUXES FOR THE OASIS SITES ESTIMATED BY THE PAIRED TOWER METHOD. SEVEN PAIRS OF EC TOWERS WERE SELECTED (DISTANCES SHOWN IN PARENTHESES)

Paired Towers	σ_r (H)	σ_r (LE)	σ_r (Fc)
5 vs. 6 (864 m)	12.55 (17%)	32.38 (17%)	1.90 (22%)
6 vs. 7 (836 m)	20.33 (32%)	47.72 (22%)	2.55 (24%)
8 vs. 9 (781 m)	20.18 (29%)	38.73 (20%)	2.38 (19%)
9 vs. 10 (972 m)	13.75 (18%)	33.72 (17%)	2.64 (17%)
5 vs. 11 (969 m)	11.50 (16%)	31.29 (17%)	1.56 (14%)
6 vs. 12 (924 m)	14.66 (22%)	36.66 (19%)	2.13 (23%)
13 vs. 15 (766 m)	15.73 (34%)	46.14 (20%)	2.40 (22%)

2) Uncertainty Estimated by Method HR05: Seven pairs of towers with distances around 780–970 m were selected for the calculation. $\sigma_r(H)$, $\sigma_r(LE)$, and $\sigma_r(Fc)$ for each paired sites were estimated and are shown in Table III. Compared with that of the ML94 method (see Table II), the results from some paired sites (e.g., 5 versus 6, 9 versus 10, and 5 versus 11) are consistent; however, relative errors are much larger for other paired sites.

As indicated in Section III-A3 , the HR05 method requires "similar environments", particularly similar surface vegetation and soil moisture for the paired sites in this study. This was rather difficult for certain sites of this oasis. For example, the vegetation status of these sites did look similar to the naked eye in the selected period. However, when we checked the NDVI values from high-resolution satellite data (a scene of advanced spaceborne thermal emission and reflection radiometer (ASTER) image on June 15), the relative variation among the 14 EC sites was as large as 8.8%. Particularly for paired sites 6 and 7, 8 and 9, and 13 and 15, the differences of NDVI were larger than 15%. Thus, the higher σ_r values for these paired towers embodied actually the effects of systematic surface differences.

V. CONCLUDING REMARKS

The EC method is now the most fundamental method for measuring fluxes, and there are no standard methods or reference samples to QC their results. An intercomparison of 20 EC sets (plus 7 LAS systems) and the intensive flux observation matrix in the HiWATER-MUSOEXE program provide a unique chance to assess the uncertainties of EC fluxes.

As aforementioned, several methods have emerged for flux uncertainty estimation. However, separating random uncertainties and systematic effects, or separating the sampling error and random instrument noise, is still very difficult in some cases. Billesbach [11] presented a selection of methods as well as their comparisons. Although most results agree well, some discrepancies are still large. We used the elementary error analysis for the Gobi intercomparison, which gave some valuable results for the estimation of both systematic and random errors (even for only the sensible heat flux), as well as a judgment of a popular method, the ML94.

The uncertainties of EC fluxes are usually the result of the stochastic nature of turbulence. Surface heterogeneity may induce more active turbulence, particularly of larger scales. Consequently, flux uncertainties over oasis surface are larger. The relative random errors of various fluxes we specified are comparable to that in the literatures. Additionally, the weakness of another popular method, the HR05, is also understandable.

Flux uncertainties, their probability distributions, and the nature of nonconstant variances are essential in the validation of model outputs, such as various fluxes derived from remote sensing and/or land surface models. There are still considerable knowledge gaps in the understanding of these uncertainties, particularly regarding practicalities in the linkage of flux data with models. The experiment of HiWATER-MUSOEXE provides also a good foundation for these studies.

REFERENCES

[1] D. D. Baldocchi, "Assessing the eddy covariance technique for evaluating carbon dioxide exchange rates of ecosystems: Past, present and future," *Glob. Change Biol.*, vol. 9, no. 4, pp. 479–492, Apr. 2003.

[2] X. Li *et al.*, "Heihe Watershed Allied Telemetry Experimental Research (HiWATER): Scientific objectives and experimental design," *Bull. Amer. Meteorol. Soc.*, vol. 94, no. 8, pp. 1145–1160, Aug. 2013.

[3] Z. Xu *et al.*, "Intercomparison of surface energy flux measurement systems used during the HiWATER-MUSOEXE," *J. Geophys. Res.*, vol. 118, no. 23, pp. 13 140–13 157, Dec. 2013.

[4] D. Lenschow, J. Mann, and L. Kristensen, "How long is long enough when measuring fluxes and other turbulence statistics?" *J. Atmos. Ocean. Technol.*, vol. 11, no. 3, pp. 661–673, Jun. 1994.

[5] A. D. Richardson, "Uncertainty quantification," in *Eddy Covariance: A Practical Guide to Measurement and Data Analysis*, M. Aubinet *et al.*, Ed. New York, NY, USA: Springer-Verlag, 2012, pp. 173–210.

[6] D. Papale *et al.*, "Towards a standardized processing of net ecosystem exchange measured with eddy covariance technique: Algorithms and uncertainty estimation," *Biogeosciences*, vol. 3, no. 4, pp. 571–583, Nov. 2006.

[7] D. Vickers and L. Mahrt, "Quality control and flux sampling problems for tower and aircraft data," *J. Atmos. Ocean. Technol.*, vol. 14, no. 3, pp. 512–526, Jun. 1997.

[8] J. Mann and D. H. Lenschow, "Errors in airborne flux measurements," *J. Geophys. Res.*, vol. 99, no. D7, pp. 14 519–14 526, Jul. 1994.

[9] P. L. Finkelstein and P. F. Sims, "Sampling error in eddy correlation flux measurements," *J. Geophys. Res.*, vol. 106, no. D4, pp. 3503–3509, Feb. 2001.

[10] D. Y. Hollinger and A. D. Richardson, "Uncertainty in eddy covariance measurements and its application to physiological models," *Tree Physiol.*, vol. 25, pp. 873–885, Jul. 2005.

[11] D. P. Billesbach, "Estimating uncertainties in individual eddy covariance flux measurements: A comparison of methods and a proposed new method," *Agric. Forest Meteorol.*, vol. 151, no. 3, pp. 394–405, Mar. 2011.

[12] M. Williams *et al.*, "Improving land surface models with FLUXNET data," *Biogeosciences*, vol. 6, pp. 1341–1359, Jul. 2009.

[13] C. J. Willmott, "Some comments on the evaluation of model performance," *Bull. Amer. Meteor. Soc.*, vol. 63, pp. 1309–1313, Nov. 1982.

[14] D. Dragoni, H. P. Schmid, C. S. B. Grimmond, and H. W. Loescher, "Uncertainty of annual net ecosystem productivity estimated using eddy covariance flux measurements," *J. Geophys. Res.*, vol. 112, no. D17, pp. D17102-1–D17102-9, Sep. 2007.